RESEARCH ARTICLE | MAY 01 2024

Experimental study on energy dissipation with different slope of downstream ogee spillway

Hajer Hussein Albank; Saleh Issa Khassaf

AIP Conf. Proc. 3091, 020037 (2024)
https://doi.org/10.1063/5.0209304

Experimental Study on Energy Dissipation with Different Slope of Downstream Ogee Spillway

Hajer Hussein Albank [1, a)] and Saleh Issa Khassaf [1)]

[1]Department of Civil Engineering, College of Engineering, University of Basrah, Al-Basrah, Iraq.

[a)] Corresponding author: *hajerhusseinedu93@gmail.com*

Abstract. A spillway acts as a safety device in a dam, and many dam failures are due to inadequate spillway capacity or incorrect spillway design. The purpose of this research was thus to investigate the impact of varying ogee spillway surface slopes with respect to energy dissipation. The body of an ogee spillway has two profiles, one downstream and one upstream of the crest: in this study, three ogee spillway models with downstream slopes of 0.6:1 (Model A), 0.8:1 (Model B), and 1:1 (Model C) were developed. The main objective was to investigate relative energy loss, and the energy dissipation downstream of the three spillway models was thus investigated by applying different flow rates. The energy dissipation was found by evaluating the difference between the energy of the spillway structure upstream (Eo) and the energy at the beginning of the hydraulic jump (E1), For each flow condition, the available energy in the various models was calculated at the toe of the spillway, close to the end of the upstream section of the hydraulic jump. A comparison between the results obtained from the physical models of different slopes was then made to determine which model dissipated more energy. The results showed that the model with a milder slope (1:1) demonstrated higher energy dissipation than that with the steeper slope (0.6:1), with relative energy dissipation being reduced over the spillway with any increase in flow rate.

INTRODUCTION

Spillways are hydraulic structures used in storage and detention dams to release excess water or floodwater that cannot be retained in within the standard storage capacity; they also act in diversion dams to allow bypass of flows that exceed those suitable for the relevant diversion system [1]. The ogee-crested spillway is the most frequently used type of spillway worldwide due to its capacity to pass flow efficiently and safely when correctly designed and constructed [2]. The ogee spillway's nappe trajectory varies with head (Hd), with a crest shape generated based on specific head or discharge [3]. One of the most significant functions of a dam is energy dissipation, and the majority of researchers have thus focused their studies on the utilisation of energy-dissipating structures downstream of both spillways and dams. In order to dissipate extra energy, energy-dissipating structures, such as hydraulic jumps, stilling basins, roller buckets, and ski jump buckets, are typically built at the end of spillway discharge channels. These energy dissipation devices dissipate the kinetic energy of excess flooding with the help of various devices at the toe portion of the spillway, assisting in the achievement of consistent flow at the river's downstream side in a manner that reduces erosion damage at the downstream end: an ogee spillway can dissipate up to 80.24% of its energy using a combination of a basic roller bucket, steps, and a stilling basin mechanism [4].

Any sudden transition from a high-velocity flow to a slower-moving flow is known as a hydraulic jump [5], and such hydraulic jumps are commonly necessary for the completion of the energy dissipation task. Tailwater depth can, however, have a major impact when a hydraulic jump is generated in a channel, and variations in depth can move the formed jump upstream or downstream [6]. The plain and slotted roller bucket models used in the spillway of the Omkareshwar and Teesta low dams were studied by Bhosekar *et al.* (2012) [7]: according to their investigation, as the surface and ground rollers were not properly formed, the roller bucket's performance was unsatisfactory across the board for all types of discharges. Al Zubaid *et al*. (2016) [8] instead investigated the hydraulic performance and efficiency of direction diverting blocks (DDBs) fixed to the surface of an ogee spillway; their results showed that the DDBs can be successfully used to lower the energy of the flow downstream of the spillway, allowing for a shorter

6th International Conference on Engineering Sciences – ICES2022
AIP Conf. Proc. 3091, 020037-1–020037-9; https://doi.org/10.1063/5.0209304

stilling basin. Furthermore, as the number of blocks and rows increased and the block apex angle decreased, more energy was lost. The main objectives of this paper are thus to study energy dissipation and investigate the effect of the downstream slopes of the ogee spillway on relative energy loss, following on from the previous investigations.

DESIGN OF AN OGEE SPILLWAY

USBR and USACE methods involve selecting a design head that is smaller than the maximum head to compute the spillway crest shape. The sub-atmospheric pressure on the face of the spillway never exceeds about one-half of the design head when H_{max}/H_d does not exceed 1.33: thus, as the maximum head expected was 4.5 cm above crest level, a design head of 3.5 cm was set.

Once the design head was determined, the actual shape of the spillway crest upstream and downstream of the apex was specified using the standard WES ogee spillway shape (USACE 1985, hydraulic design chart 111-16).
The upstream crest profile details are tabulated in Table 1.

TABLE 1. Details of spillway model A

Slope of the upstream	Vertical
Height of the spillway [P]	450 mm
Design head [H_d]	35 mm
First radius of ogee curve [R_1= 0.5 H_d]	17.5 mm
Second radius of ogee curve [R_2= 0.2 H_d]	7 mm
Third radius of ogee curve [R_3=0.04 H_d]	1.4 mm
Distance between crest axis and the end of the first ogee curve [a = 0.175 H_d]	6.125 mm
Distance between crest axis and the end of the third ogee curve [b = 0.282 H_d]	9.87 mm
The radius of toe =$\frac{P}{4}$	110 mm

Equation 1 was then used for the design of the downstream crest profile (USACE – WES (1985)):

$$X^n = K.H_d^{n-1}.y \tag{1}$$

where H_d , is the design head above the crest, X and Y are the coordinates of the crest profile with their origins at the highest point of the crest, and K and n are constants dependent on the upstream slope.

For the vertical upstream face, the constants K and n are 2 and 1.85 respectively.

In order to find the maximum x where the downstream crest profile ends, it is necessary to determine $\frac{dy}{dx}$ and to set this equal to the downstream slope of the ogee spillway:

$$x^{1.85} = 2\ H_d^{\ 0.85}.\ y$$

$$y = \frac{x^{1.85}}{5.8008} \rightarrow \frac{dy}{dx} = \frac{1.85}{5.8008}\ x^{0.85} \rightarrow \frac{1}{0.6} = 0.3189\ x^{0.85}$$

$$x = 6.9974 \text{ cm}$$

As the downstream crest profile ends, a straight line of inclination 1.0V:0.6H can be established to maintain the spillway height, as shown in Fig. 1a. The designs of models B and C were executed in a similar manner, as shown in Figs. 1b and 1c.

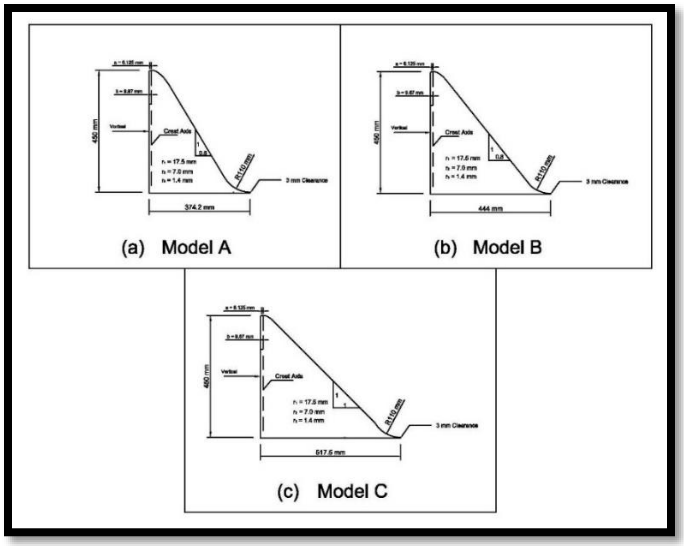

FIGURE 1. Sketches of experimental ogee models

MATERIALS AND METHODS

Experimental flume

The flume was created in the hydraulic engineering laboratory at the University of Basra. All tests were carried out in a 10 metres-long rectangular flume of 78 cm * 80 cm cross-section. The flume walls were made of plexiglass, while the bed was made of painted steel. The flume's bed was kept on a horizontal slope as shown in Fig. 2, while the flume itself was divided into three sections, the first of which was an input tank. The second section was the working section of the flume consisting of a harp-crested rectangular weir 73.2 cm wide and 45 cm tall, which was used to measure flow discharge, with gravel and screens used to help dissipate the extra energy of flow by distributing the flow uniformly across the entire width of the flume; such screens act as wave breakers and provide a smooth water surface profile before the spillway. The third section of the flume was a reservoir that provided water by recirculating flume output to create a closed water system using a centrifugal pump of a maximum capacity of about 1,200 l/min attached to an electric motor. A point gauge was used to measure the depth of flow by placing the needle tip of the point gauge on the water surface and reading the level on the ruler. The water depth upstream varied between 10 mm and 45 mm above the crest level, and the minimum and maximum discharges were 1.276 l/sec and 18.194 l/sec, respectively. At these water depths within the flume, spillway models were thus installed, and each spillway model was subjected to ten test runs.

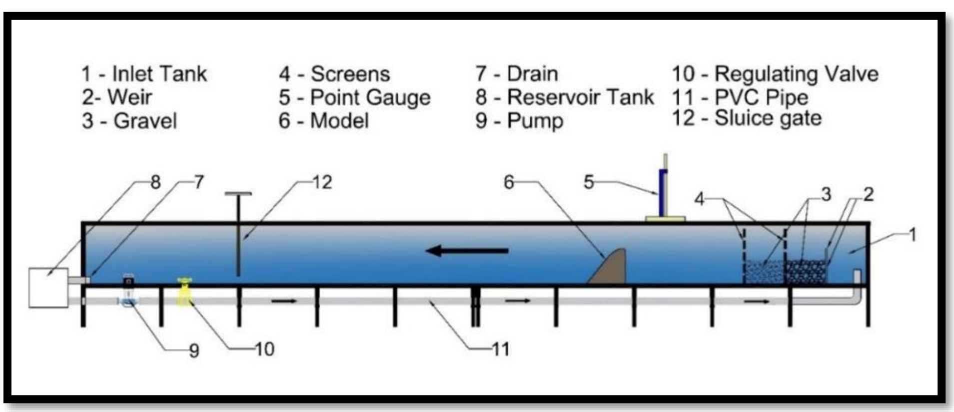

FIGURE 2. Detailed drawing of a laboratory flume

Experimental models

The models were created from well-painted wood structures, with water-resistant varnish used to prevent the wood from changing volume as a result of water absorption. Each structure was then covered with a galvanized steel sheet and painted with a thin layer of epoxy resin.

METHOD

The following laboratory technique was followed for all test runs across the three ogee spillway models:

- The flowrate of the test run was determined by adjusting the pumps' control valve and measuring the water head above the weir's crest.
- The approach depth $y_{o.}$ at a distance 2.5* maximum head before the ogee crest axis was measured.
- The hydraulic jump's position and shape (downstream the model) were controlled by a sluice gate controlling the flow area. The depth of the tailwater was increased gradually until the front of the jump went upstream to the spillway toe, as shown in Fig. 3.

FIGURE 3. Flow over ogee spillway and jump location

- The water's sequent depth y_2 was then measured.
- The Froud number of the sequent depth (Fr_2) was calculated using Eq. (2):

$$F_r = \frac{v_2}{\sqrt{g y_2}} \tag{2}$$

- The water's initial depth y_1 was calculated using Belanger's formula:

$$y_1 = \frac{y_2}{2}\left(\sqrt{1 + 8\,Fr_2^2} - 1\right) \tag{3}$$

though the measured values are always smaller than the ones obtained using Belanger's formula as seen in Eq. (3) [9].

- Energy equations were applied to determine the percentage of energy dissipated, as shown in Eq. (4), (5), and (6):

$$E_o = y_o + \frac{v_o^2}{2g} \tag{4}$$

$$E_1 = y_1 + \frac{v_1^2}{2g} \tag{5}$$

$$\frac{E_L}{E_o} = \frac{E_o - E_1}{E_o}\ \% \tag{6}$$

where:
E_o = energy at the crest of the spillway (L), E_1 = energy at the beginning of the hydraulic jump (L,
V_o = Upstream velocity (L/T), V_1 = downstream velocity (L/T) g = acceleration due to gravity (L/T^2), and
$\frac{E_L}{E_o}$ % = Relative energy dissipation between U/S and D/S of ogee spillway.
Details of the energy lines are shown in Fig. 4.

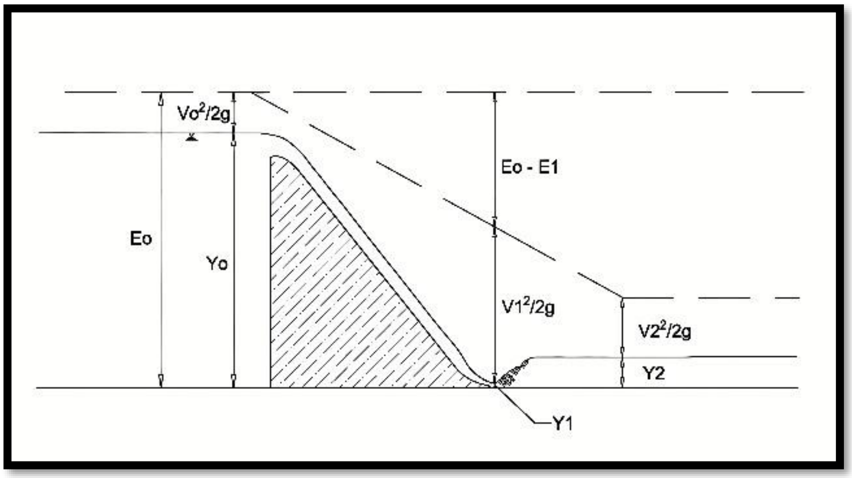

FIGURE 4. Details of energy lines

DIMENSIONAL ANALYSIS TECHNIQUES

Dimensional analysis is a mathematical approach used to investigate hydraulic problems or phenomena that have a variety of physical measures in detail, and it can thus be used to form associations by recognising the relevant fundamental dimensions [10]. Dimensional analyses were used in this research to analyse the flow of water over the ogee spillway to obtain the important parameters to be studied in the experimental work and to develop a new formula for such investigation. The parameters that affect this study topic are thus outlined in Table 2.

TABLE 2. Variables considered in this study and their dimensions

VARIABLES	MEANING	DIMENSION
	FLUID PROPERTIES	
ρ	The density of the fluid	ML^{-3}
μ	Dynamic viscosity of the fluid	$ML^{-1}T^{-1}$
	FLOW CHARACTERISTICS	
g	Gravitational acceleration	LT^{-2}
E_o	Specific energy	L
E_L	Energy loss	L
	GEOMETRICAL CHARACTERISTICS	
S_d	The slope of the downstream	-
R	Radius of crest	L

ENERGY DISSIPATION ANALYSIS

The initial stage in formula development was to choose parameters that influence energy dissipation flow significantly. The input parameters were the focus of this study in order to keep correlations as simple as possible, as indicated below:

$$F(\rho, \mu, g, E_o, E_L, q, R, S_d) = 0 \quad (4)$$

Using the π- theorem [11], and the M-L-T system where:
m = 8 (number of variables)
n = 3 (number of primary units involved in the problem)
The number of dimensionless π- theorem values = m-n = 8 - 3 = 5
Taking the common variables (ρ, g, R) as repeating variables, equation (4) can thus be written as the Buckingham theorem:

$$F(\pi_1, \pi_2, \pi_3, \pi_4, \pi_5) = 0 \tag{5}$$

Where:
$\pi_1 = \rho^{a1} \; g^{b1} \; R^{c1} \; E_o$ $\quad \pi_4 = \rho^{a4} \; g^{b4} \; R^{c4} \; q$
$\pi_2 = \rho^{a2} \; g^{b2} \; R^{c2} \; E_L$ $\quad \pi_5 = \rho^{a5} \; g^{b5} \; R^{c5} \; S_d$
$\pi_3 = \rho^{a3} \; g^{b3} \; R^{c3} \; \mu$

By taking each π term and expressing it in dimensional form,
$M^0 L^0 T^0 = [M L^{-3}]^{a1} \; [L T^{-2}]^{b1} \; [L]^{c1} \; [L]$
For M: $a^1 = 0$
For L: $-3a^1 + 2b^1 + c^1 = 0 \rightarrow c^1 = 0$
For T: $-2 b^1 = 0$

So that $\pi_1 = \frac{E_o}{R}$.

In the same way,
$\pi_2 = \frac{E_L}{R} =$ $\pi_3 = \frac{\mu}{\rho q} = Re$ $\quad \pi_4 = \frac{q}{g^{1/2} R^{3/2}} = Fr_o$ $\quad \pi_5 = S_d$

$\pi_2 / \pi_1 = \frac{E_L}{E_o}$

The functional relationship may thus be written as

$$\frac{E_L}{E_o} = f\,(Fr_o, Re, Sd) \tag{6}$$

However, Re can be neglected and therefore

$$\frac{E_L}{E_o} = f\,(Fr_o, Sd). \tag{7}$$

RESULTS AND DISCUSSION

Discussing and analysing the results acquired from the laboratory data is a most important step in understanding the crucial factors that affect energy dissipation. All experiments was performed at the laboratory of hydraulics in the civil engineering department at the University of Basrah, and the measurements and outputs for all experimented models are displayed in Table 3.

The relative energy dissipation became higher as the slope of the spillway became milder, and vice versa. The relative energy dissipation for a spillway with a downstream slope 1:1 (Model C) was thus higher than that of a spillway with a downstream slope of 0.8:1 (Model B) by 11 % at maximum, and by 21.4% more at maximum as compared to a spillway with a downstream slope of 0.6:1 (Model A). Figure 5 shows the relationship between flowrate per unit width (q) and relative energy dissipation: the three curves tend to become horizontal as the passing flowrate increases, which means that no major reduction in relative energy dissipation is expected if the flowrate increases further.

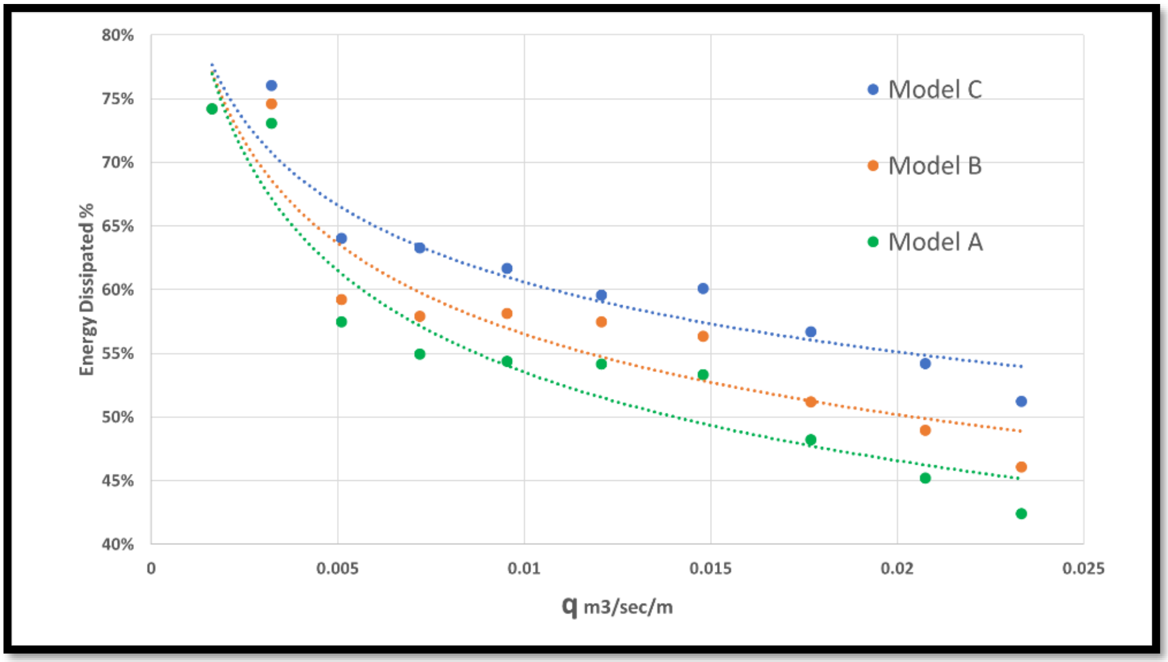

FIGURE 5. Relationship between energy dissipated and discharge per unit width

The relation between Froude number at approach depth Fr_o and relative energy dissipation is shown in Fig. 6. This is clearly shows that the energy dissipation decreases as the Froude number approaches the critical limit.

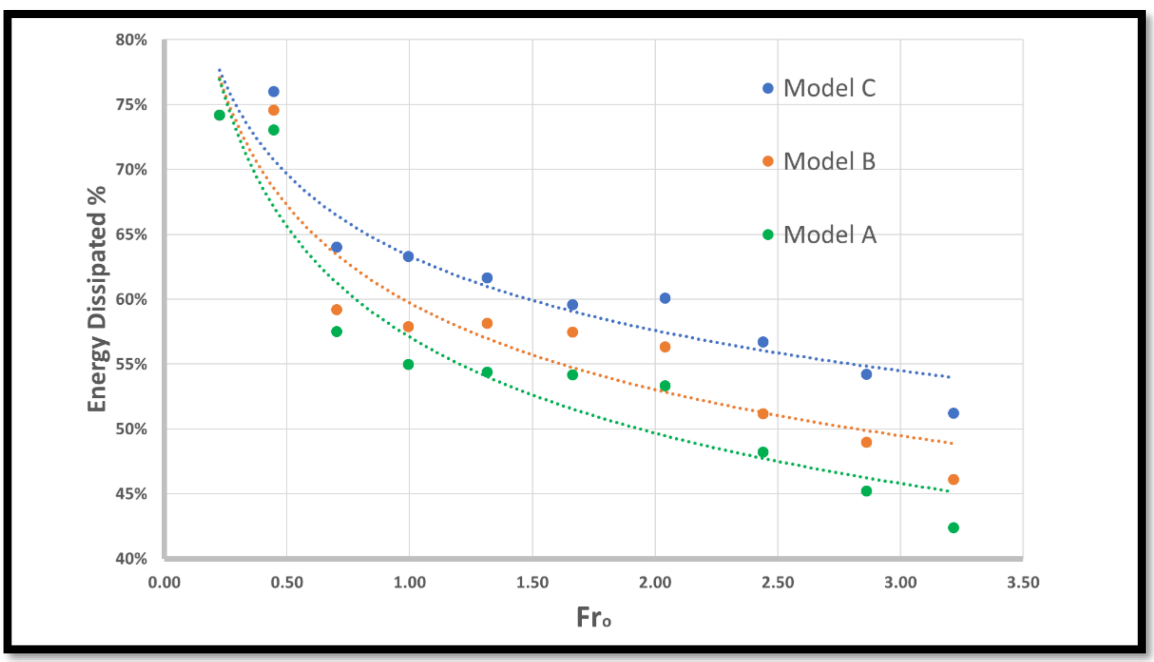

FIGURE 6. Relationship between energy dissipated and Fr_o

TABLE 3. Laboratory data describing energy dissipation for various discharges and models.

Model Description	Unit Discharge q ($m^3/s/m$)	Approach depth y_o (m)	Approach energy E_o (m)	Sequent Depth y_2 (m)	Froude Number Fr_2	Pre Jump depth y_1 (m)	Pre jump Energy E_1 (m)	Energy Dissipation EL/E_o (%)
Model A Vertical Upstream; Downstream slope 0.6H:1V	0.2257	0.460	0.4614	0.0220	0.160	0.0011	0.1191	74%
	0.4452	0.465	0.4670	0.0310	0.189	0.0021	0.1258	73%
	0.7029	0.469	0.4727	0.0440	0.176	0.0026	0.2009	57%
	0.9940	0.474	0.4783	0.0530	0.189	0.0035	0.2155	55%
	1.3154	0.478	0.4836	0.0610	0.202	0.0046	0.2207	54%
	1.6646	0.481	0.4887	0.0685	0.215	0.0058	0.2241	54%
	2.0398	0.484	0.4936	0.0760	0.225	0.0071	0.2305	53%
	2.4395	0.488	0.4988	0.0855	0.226	0.0080	0.2583	48%
	2.8625	0.491	0.5041	0.0940	0.230	0.0091	0.2762	45%
	3.2169	0.494	0.5082	0.1010	0.232	0.0099	0.2927	42%
Model B Vertical Upstream; Downstream slope 0.8H:1V	0.2257	0.460	0.4614	0.0220	0.160	0.0011	0.1191	74%
	0.4452	0.465	0.4670	0.0305	0.193	0.0021	0.1187	75%
	0.7029	0.469	0.4727	0.0435	0.179	0.0026	0.1928	59%
	0.9940	0.474	0.4783	0.0520	0.194	0.0037	0.2014	58%
	1.3154	0.478	0.4836	0.0595	0.210	0.0048	0.2024	58%
	1.6646	0.481	0.4887	0.0670	0.222	0.0061	0.2078	57%
	2.0398	0.484	0.4936	0.0745	0.232	0.0073	0.2156	56%
	2.4395	0.488	0.4988	0.0840	0.232	0.0082	0.2435	51%
	2.8625	0.491	0.5041	0.0920	0.237	0.0094	0.2572	49%
	3.2169	0.494	0.5082	0.0990	0.239	0.0103	0.2739	46%
Model C Vertical Upstream; Downstream slope 1H:1V	0.2257	0.460	0.4614	0.0220	0.160	0.0011	0.1191	74%
	0.4452	0.465	0.4670	0.0300	0.198	0.0022	0.1120	76%
	0.7029	0.469	0.4727	0.0420	0.189	0.0028	0.1701	64%
	0.9940	0.474	0.4783	0.0500	0.206	0.0039	0.1755	63%
	1.3154	0.478	0.4836	0.0580	0.218	0.0051	0.1854	62%
	1.6646	0.481	0.4887	0.0660	0.227	0.0062	0.1975	60%
	2.0398	0.484	0.4936	0.0725	0.242	0.0077	0.1971	60%
	2.4395	0.488	0.4988	0.0810	0.245	0.0088	0.2160	57%
	2.8625	0.491	0.5041	0.0890	0.250	0.0100	0.2308	54%
	3.2169	0.494	0.5082	0.0960	0.250	0.0108	0.2478	51%

CONCLUSIONS

The experiments showed that the relative energy dissipation became greater as the downstream slope became milder. A spillway with downstream slope with a 1:1 (Model C) ratio has a relative energy dissipation 11% greater than that of on with a 0.8:1(Model B) ratio and 21.4 % greater than of one with a 0.6:1(Model A) ratio.

It was observed that the relative energy dissipation decreased with the increase in Froude number at the approach depth Fr_o.

The current investigation thus highlights the sensitivity of relative energy loss to the design head, as the reduction in relative energy loss was most obvious when the depth of water over the spillway's crest y_o took values greater than the design head.

REFERENCES

1. U.S. Bureau Of Reclamation, Design of small dams (U.S. Government Printing Office, A Water Resources Technical Publication, 1987), pp. 339-4
2. J. R. Mohammed, B. M. A. Noori, I. A. Hussein, Journal of Duhok University. **20,** 638-653 (2017).
3. A. Chadwick, j. Morfett and M. Borthwick, *Hydraulics in Civil and Environmental Engineering* (CRC Press, London 2021). pp. 652
4. P. B.Nangare, A. A.Patil and S. A.Pande, International Journal of Engineering Research in Mechanical and Civil Engineering, 94-100 (2018).
5. H. Chanson, J. Irrig. Drain. Eng. **138**, 382-385 (2012).
6. G. A. Hinge, S. Balkrishna, and K. C. Khare, Aust. J. Basic Appl. Sci. **4,** 3261-3267 (2010).
7. V. Bhosekar, International Journal of Water and Energy. **69**, 47-54 (2012).
8. R. Z Al Zubaidy, K. I Khedher and A. N Darweesh, J. of Engineering. **22**, 77–88 (2016).
9. D. A. Al Ghwail, S. Stević and M. A. Abourohiem, Journal of the Croatian Association of Civil Engineers. **70**, 377-391 (2016).
10. M. B. Rashak and S. I. Khassaf, Journal of Water and land development. 1–9 (2021).
11. H. I. Al shaikhli and S. I. Khassaf, International Journal of Aquatic Science .**12**, 98-104 (2021).